

## THE MAGNETIC ROTATION SPECTRUM AND HEAT OF DISSOCIATION OF THE LITHIUM MOLECULE

BY F. W. LOOMIS AND R. E. NUSBAUM  
THE UNIVERSITY OF ILLINOIS

(Received August 20, 1931)

## ABSTRACT

The magnetic rotation spectrum of the green,  ${}^1\Pi-{}^1\Sigma$ , band system of  $\text{Li}_2$  has been observed and used to locate bands with high quantum numbers and so to obtain an accurate value for the heat of dissociation of the normal  $\text{Li}_2$  molecule, yielding  $D_0'' = 1.14 \pm 0.03$  volts. The spectrum is less simple than in  $\text{Na}_2$ , for instance, in that we observe not only a strong line at the head of each band, but also a few lines of the  $P$  and  $R$ , but not  $Q$ , branches. An improved method of plotting Franck-Condon diagrams is illustrated.

IT HAS been shown by Loomis<sup>1</sup> in the case of sodium that the magnetic rotation spectrum affords a very powerful method of attack on the analysis of the vibrational levels of a molecule, and particularly on the extension towards higher levels which is necessary for good estimation of the heat of dissociation. The reason for this is that the magnetic rotation spectrum is a much simplified version of the absorption spectrum with, consequently, much less overlapping of bands, so that the bands of high quantum numbers which are weak and, in this type of molecule at least, lie among stronger bands, can be identified and measured.

According to the simple theory of the magnetic rotation spectrum,<sup>2</sup> the intensities of lines in the  $P$  and  $R$  branches are proportional to the intensities of the corresponding absorption lines, times the Zeeman splitting, times some function of the Zeeman pattern. The  $Q$  branch should not appear in magnetic rotation. The Zeeman splitting falls off so rapidly as one proceeds from the origin, roughly as  $1/J^2$ , that only the lines nearest the origin appear at all. In fact, in sodium, each band appears as just one line, at the head, made up, in reality of a group of strong  $R$  lines. The corresponding  $P$  lines of low  $J$  are spread out and do not appear under the usual conditions. Roughly, it may be said that the magnetic rotation spectrum is rather like an absorption spectrum with an extremely low effective temperature as far as molecular rotation is concerned, but not as to vibration.

Now a vibrational analysis of the spectrum of  $\text{Li}_2$  has already been made by Wurm,<sup>3</sup> on the basis of absorption measurements, and a value, 1.69 volts, deduced therefrom as the heat of dissociation; but the extrapolation is so long that no particular reliance can be placed on the result. The authors have therefore thought it desirable to study the magnetic rotation spectrum of

<sup>1</sup> Loomis, Phys. Rev. **31**, 323 (1928).

<sup>2</sup> Kemble, National Research Council Bulletin **57**, Chapter VII

<sup>3</sup> Wurm, Naturwiss. **16**, 1028 (1928).

$\text{Li}_2$ , with a view to obtaining a dependable measurement of the heat of dissociation, and also of gaining further information about certain other points which will be discussed below.

While this research was in progress Professor Bartlett and Mr. Furry of this department carried through a computation of the heat of dissociation by quantum theoretical methods which are much more precise than that which had previously been used by Delbrück<sup>4</sup> for the same purpose. Delbrück had obtained the value 1.4 volts. Bartlett and Furry<sup>5</sup> found 1.12 volts.

Because of the high temperatures required to yield enough lithium vapor, it was necessary to use a somewhat modified experimental method. The lithium was contained in a nickel tube 100 cm long by 2.5 cm diameter, with a side tube fused on near one end for evacuation and with glass windows at the ends attached with sealing wax. As temperatures near the melting point of nickel were to be used, it was necessary to have a method of heating which

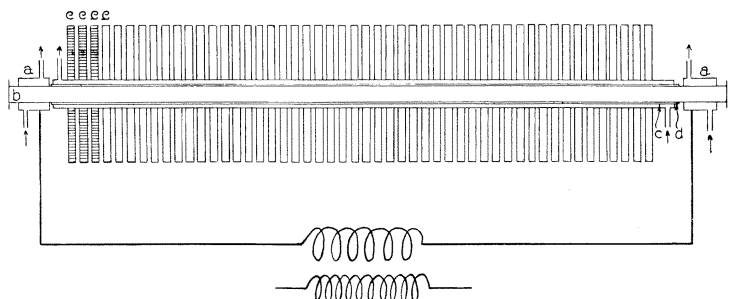


Fig. 1. Diagram of apparatus. *a, a*: cooling jackets. *b*: nickel absorption tube. *c*: water layer. *d*: asbestos layer, *e, e, e*: pancake coils.

allowed precise temperature control. For this purpose a large current (about 150 amperes) was sent along the nickel tube itself from a step down transformer governed by an induction regulator. Contacts were made to the tube by special water cooled electrodes which served the double purpose of preventing local heating at the contacts and of keeping the windows cool.

The magnetic field was produced by an air-cooled solenoid consisting of 50 coaxial pancake coils, each made of 90 turns of half-inch copper ribbon 0.05 cm thick and insulated by winding half-inch asbestos ribbon between the turns of the copper. The solenoid could carry a steady current of about 30 amperes and produced a field of some 1800 gauss. The nickel tube became saturated at low fields and did not act appreciably as a magnetic shield to the lithium vapor. The solenoid was protected from the heat of the nickel tube by a thin layer of water flowing between two coaxial brass tubes between the nickel tube and the solenoid. A diagram of the apparatus is shown in Fig. 1.

Usually sunlight was used as a source. It was reflected from a heliostat, through the first nicol, the tube of lithium vapor and the second nicol and focussed with a lens onto the slit of the spectrograph, a Hilger E1 with glass

<sup>4</sup> Delbrück, *Ann. d. Physik* **5**, 36 (1930).

<sup>5</sup> Bartlett and Furry, *Phys. Rev.* **37**, 1712A (1931).

optical system. Before the magnetic field was turned on, the nicols were set for extinction. This could only be done with success when the beam had been restricted by shields so that no part of the light was reflected from the walls of the tube. When the field was turned on, the spectrum appeared and could be photographed with exposures of from fifteen minutes to some ten hours, according to slit width, vapor density, etc.

There are two band systems of  $\text{Li}_2$  in the visible, which have the  ${}^1\Sigma$  ground state of the molecule in common.<sup>6,7,8</sup> The green system is a  ${}^1\Pi - {}^1\Sigma$  transition, the red one is  ${}^1\Sigma - {}^1\Sigma$ , just as in the case of sodium. A photograph of almost the whole of the green system is reproduced in Fig. 2a; an enlarged portion of it, near the system origin, being shown in Fig. 2b. Attempts to find a magnetic rotation spectrum in the red have been unsuccessful. Unfortunately we are unable to say whether this is due to nonexistence of the spectrum or our inability, being limited by the melting point of nickel, to get sufficient

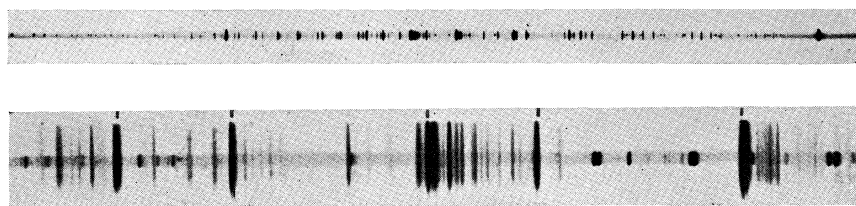


Fig. 2. a. Whole green magnetic rotation system of  $\text{Li}_2$ . b. Enlarged portion near origin. Short lines are iron comparison.

density of lithium molecules. It would be an interesting point to settle. There is a strong red magnetic rotation spectrum<sup>9</sup> of sodium in the region of the  ${}^1\Sigma - {}^1\Sigma$  system but all attempts to correlate it with the absorption system have hitherto failed. Moreover it is theoretically not to be expected that a  ${}^1\Sigma - {}^1\Sigma$  transition should have a magnetic rotation spectrum. We find that the magnetic rotation spectrum is stronger the lower the pressure of residual gas; and consequently we work with as low a pressure as is compatible with not fogging the windows. This is about 0.5 mm. The optimum temperature, or density of vapor, depends on the portion of the spectrum in which one is most interested. Too much vapor wipes out the spectrum by reabsorption.

On account of the favorable intensity distribution, discussed above, it was comparatively easy to extend the progressions of bands, in both directions, to where they completely disagreed with Wurm's<sup>3</sup> and with Harvey and Jenkins's<sup>8</sup> formulas. As convergence is approached however the process of measuring bands and assigning quantum numbers becomes difficult and it is necessary to proceed with caution. It is worth while to consider the reasons for this, as they constitute the essential limitations on the extent to which con-

<sup>6</sup> Wurm, *Zeits. f. Physik* **58**, 562 (1929).

<sup>7</sup> Wurm, *Zeits. f. Physik* **59**, 35 (1929).

<sup>8</sup> Harvey and Jenkins, *Phys. Rev.* **35**, 789 (1930).

<sup>9</sup> R. W. Wood, *Proc. Am. Acad.* **42**, 235 (1906); *Astrophys. J.* **30**, 339 (1909).

vergence can be approached, and hence on the accuracy with which heats of dissociation can be deduced from band spectra, at least of this type.

One difficulty is that, as convergence is approached, it ceases to be possible to represent the levels by any simple formula, so that extrapolation becomes difficult. If the spectrum is sufficiently sharp, however, this can be overcome with patience; since, when the correct assignments are found, the combination relations accurately check them.

Another difficulty is that we are not here dealing with a simple extreme case, such as iodine, where one can follow one single  $v'$  progression all the way to convergence because the Franck-Condon parabola lies along the axis of  $v'$  (or  $T'$ ). Rather, in order to reach high values of  $v'$  we have to be able to assign the high numbered bands to the usual two dimensional array and moreover the weak bands with high  $v'$ , in which we are most interested, lie among the strong bands near the system origin. That this is so can be readily seen by inspection of the improved Franck-Condon diagram in Fig. 7. Note that, as explained below, the frequency of each band is obtained by projecting it back at  $45^\circ$  onto the  $T'$  axis. This difficulty is the real limitation on the extent to which the absorption spectrum can be followed, as these weak bands are completely covered by the strong ones near the system origin. The principal advantage of the magnetic rotation method is that it localizes the strong bands so sharply that the weak ones can be picked out between them.

A more serious limitation is the rapidly diminishing intensity of the bands with increasing  $v'$ . The bands with highest  $v'$  lie on the left arm of the Franck-Condon parabola and correspond to transitions between the steep parts of the potential energy curves. Now with increasing  $v'$  the steep left side of a curve becomes steeper and the flat right side becomes very much flatter and correspondingly the time the vibrator spends in turning around at the left end becomes less while that spent at the right end becomes very much greater. The result is that the favoring of the right arm of the parabola over the left arm, which is present at all levels, becomes much accentuated at high quantum numbers and the transitions corresponding to the left arm of the parabola become very weak. This is often a controlling factor in intensity distribution, both in absorption and emission (fluorescence) spectra. This explanation can easily be restated in quantum mechanical form.

Contrary to what one might at first suppose, the Boltzmann factor is not the most important limitation on the intensities of the bands needed for estimation of the heat of dissociation. These bands have high  $v'$  but not particularly high  $v''$ , see Fig. 7, and it is  $v''$  which, in absorption and magnetic rotation, is controlled by the Boltzmann factor. The right arm of the Franck-Condon parabola extends to much higher values of  $v''$  than are found on the left arm.

Two further factors probably contribute to the difficulty of measuring bands with high  $v'$ . First, the heads of these bands tend to become somewhat diffuse, as  $B'$  decreases rapidly and  $|C|$  increases, bringing the head to the origin where the line intensity is zero, and carrying the region of maximum intensity away from it. Second, there should be trouble due to an overlapping continuum which the Franck-Condon curve runs into. See Fig. 7.

The spectra in Fig. 2 are in one respect distinctly different from any previously observed. Whereas Wood's<sup>9</sup> magnetic rotation spectra of sodium consist of sharp lines, which have been interpreted, as explained above, as due to the piling up of strong *R* lines at the head of each band, here many of the strong lines show shading toward the red, or even series of lines running off to the red. Theoretically these should be the lines of the *P* branch and this we have confirmed by measuring them and comparing them with the absorption lines in the bands studied by Wurm<sup>6</sup> and by Harvey and Jenkins.<sup>8</sup> In each case we were able to show that the *P* and *R* lines were present and the *Q* lines absent; which is as it should be. It is interesting to see the theory of the formation of the line magnetic rotation spectrum confirmed in detail because, although it is intrinsically plausible, it has always seemed a little hard to reconcile with the sharpness of the lines. The present method of observation with a long tube of vapor tends to enhance these weak lines relatively to the strong ones because the strong ones are cut down by absorption.

All bands to which quantum numbers have been assigned are shown in Table I. The structure lines which shade off from these band heads are not included, nor are a number of weak heads which could not with certainty be distinguished from the structure lines. All distinct heads are included. Columns 1 and 2 give the quantum numbers assigned. Where a prime is attached the band is due to the isotopic molecule Li<sup>7</sup> Li<sup>6</sup>. Column 3 shows the very roughly estimated photographic intensity. Column 4 shows the observed frequency; column 5 the frequency calculated by Eq. (1) and column 6 the difference, observed frequency minus calculated.

It will be noted that bands due to the molecule Li<sup>7</sup> Li<sup>6</sup> are present. In many cases they are strong enough so that their *P* branches show. Now Li<sup>6</sup> is about 1/16 as abundant as Li<sup>7</sup>, so that these molecules should be about 1/8 as abundant as Li<sup>7</sup> Li<sup>7</sup>. There is a slight, but very slight, hope that if we can later photograph this spectrum with higher dispersion we may be able to detect bands due to the molecules Li<sup>6</sup> Li<sup>6</sup> which are 1/256 as abundant as Li<sup>7</sup> Li<sup>7</sup>, and possibly even detect the alternating intensities, or the absence of alternate lines which has been predicted on the basis of absence of hyperfine structure<sup>10</sup> of the atomic lines.

Since our measurements extend to bands with  $v'$  and  $v''$  so high that Wurm's and Harvey and Jenkins' formulas completely fail, it was necessary for a good estimate of the heat of dissociation to construct a new formula to represent all the bands. Eq. (1)

$$\nu = 20439.40 + 269.69(v' + \frac{1}{2}) - 2.744(v' + \frac{1}{2})^2 - 0.0637(v' + \frac{1}{2})^3 \\ - [351.60(v'' + \frac{1}{2}) - 2.590(v'' + \frac{1}{2})^2 - 0.0097(v'' + \frac{1}{2})^3] \quad (1)$$

was found to fit all the bands with  $v' < 12$  rather well, and the residuals in Table I are calculated with reference to it. It appears however that bands with  $v' \geq 12$  show systematic and large deviations from this formula. Another third degree equation,

<sup>10</sup> Schüler, Zeits. f. Physik **66**, 431 (1930).

TABLE I.

$v'$	$v''$	Intensity	$\nu$ observed	$\nu$ calc. by (1)	observed- calculated
11	2	3	22218.92	22218.37	+0.55
7	0	0	22105.34	22105.69	-0.35
12	3	3	22056.62	22058.88	-2.26
10	2	6	22032.75	22032.20	+0.55
8	1	6	21973.67	21972.84	+0.83
13	4	3	21887.89	21894.49	-6.60
6	0	6	21882.43	21883.80	-1.37
11	3	6	21882.43	21882.58	-0.15
9	2	6	21837.64	21836.52	+1.12
7	1	15	21759.13	21759.30	-0.17
12	4	3	21726.92	21728.47	-1.55
14	5	0	21711.58	21724.91	-13.33
5	0	3	21652.90	21653.94	-1.04
8	2	6	21632.94	21631.73	+1.21
13	5	3	21563.84	21569.53	-5.69
11	4	6	21551.15	21552.17	-1.02
6	1	40	21538.15	21537.41	+0.74
9	3	6	21501.74	21500.73	+1.01
4	0	30	21418.22	21416.48	+1.74
7	2	30	21418.22	21418.19	+0.03
10	4	3	21367.13	21366.00	+1.13
5	1	40	21307.93	21307.55	+0.38
8	3	10	21295.48	21295.94	-0.46
11	5	6	21226.43	21227.21	-0.78
3'	0'	5	21198.91	21200.11	-1.20
6	2	8	21195.97	21196.30	-0.33
3	0	15	21171.42	21171.82	-0.40
4'	1'	20	21092.51	21092.86	-0.35
7	3	30	21081.68	21082.40	-0.72
12	6	30	21081.68	21084.05	-2.37
4	1	40	21069.55	21070.09	-0.54
10	5	0	21041.01	21041.04	-0.03
5	2	15	20966.64	20966.44	+0.20
8	4	15	20966.64	20965.53	+1.11
2'	0'	10	20939.54	20939.16	+0.38
2	0	100	20919.78	20920.33	-0.55
11	6	0	20907.05	20907.75	-0.70
6	3	5	20858.69	20860.51	-1.82
3'	1'	10	20839.65	20838.93	+0.72
3	1	100	20825.08	20825.43	-0.35
7	4	5	20751.12	20751.99	-0.87
4	2	10	20729.28	20728.98	+0.30
10	6	5	20722.40	20721.58	+0.82
1'	0'	15	20670.39	20671.21	-0.82
1	0	40	20663.32	20662.40	+0.92
8	5	30	20638.98	20640.57	-1.59
2'	1'	3	20576.40	20578.41	-2.01
2	1	50	20571.73	20573.94	-2.21
0	0	100	20397.79	20398.40	-0.61
0'	0'	50	20395.24	20396.68	-1.44
1	1	8	20315.32	20316.01	-0.69
2	2	3	20232.97	20232.83	+0.14
3	3	3	20149.02	20148.53	+0.49
4	4	0	20062.06	20062.78	-0.72
0	1	12	20052.24	20052.01	+0.23
1	2	12	19974.93	19974.90	+0.03
5	5	12	19974.93	19975.28	-0.35
3	4	0	19815.91	19818.12	-2.21
4	5	0	19738.10	19737.82	+0.28
0	2	12	19708.61	19710.90	-2.29
0'	2'	0	19678.51	19678.17	+0.34
1	3	6	19637.74	19639.11	-1.37
2	4	1	19567.22	19566.63	+0.59

TABLE I. (Cont.)

$v' - v''$		Intensity	$\nu$ observed	$\nu$ calc. by (1)	observed- calculated
0	3	12	19374.16	19375.11	-0.95
1	4	3	19308.58	19308.70	-0.12
6	8	1	19264.23	19263.49	+0.74
2	5	3	19242.18	19241.67	+0.51
3	6	3	19174.06	19173.70	+0.36
4	7	0	19104.23	19104.45	-0.22
1	5	1	18983.49	18983.74	-0.25
2	6	1	18922.34	18922.21	+0.13
3	7	6	18859.63	18859.79	-0.16
4	8	1	18797.24	18796.17	+1.07
5	9	1	18730.83	18731.02	-0.19
1	6	0	18664.50	18664.28	+0.22
6	10	0	18664.50	18664.00	+0.50
2	7	0	18607.85	18608.30	-0.45
3	8	0	18552.16	18551.51	+0.65
4	9	0	18493.76	18493.56	+0.20
5	10	0	18433.24	18434.14	-0.90
6	11	1	18372.81	18372.92	-0.11
7	12	1	18310.53	18309.57	+0.96
3	9	1	18249.82	18248.90	+0.92
8	13	1	18241.82	18243.79	-1.97
4	10	1	18196.20	18196.68	-0.48
5	11	1	18142.51	18143.06	-0.55
6	12	0	18087.04	18087.68	-0.64
7	13	0	18029.55	18030.25	-0.70
8	14	0	17969.74	17970.43	-0.69
9	15	0	17909.48	17907.88	+1.60

$$\nu = 20440.10 + 268.09(v' + \frac{1}{2}) - 2.341(v' + \frac{1}{2})^2 - 0.0879(v' + \frac{1}{2})^3 - [351.60(v'' + \frac{1}{2}) - 2.590(v'' + \frac{1}{2})^2 - 0.0097(v'' + \frac{1}{2})^3], \quad (2)$$

was found, by least squares, which represented the higher bands adequately but was definitely inferior for the lower ones. Fig. 3 illustrates the situation. The residuals from (1) are plotted against  $v'$  and can be compared with the curve which represents (2) - (1). The value of  $D_0'$ , the energy of dissociation deduced from (1) is  $3903 \text{ cm}^{-1} = 0.48 \text{ volts}$ . That deduced from (2)  $3738 \text{ cm}^{-1} = 0.46 \text{ volts}$ . The latter should be distinctly better and may be accepted as having a probable error<sup>11</sup> of not over 0.03 volts. Hence

$$D_0'' = \nu(0, 0) + D_0' - \nu_A = 20398 + 3738 - 14904 = 9232 \text{ cm}^{-1} = 1.14 \pm 0.03 \text{ volts},^{12} \quad (3)$$

$\nu_A$  being the frequency of the resonance lines of the lithium atom. The value of  $D_0''$  calculated from direct extrapolation of the lower levels is 1.20 volt, which agrees fairly well with (3) but is much less accurate, as the extrapolation is longer.

It will be noted that this new and accurate value of the heat of dissociation of the normal lithium molecule agrees surprisingly well with Bartlett and Furry's<sup>5</sup> quantum mechanical calculation,  $D_0'' = 1.12 \text{ volts}$ , but differs con-

<sup>11</sup> That is, we believe the true value is at least as likely to be within the range 1.11-1.17 volts, as outside it.

<sup>12</sup> The corresponding value of the energy of dissociation reckoned from the bottom of the potential energy curve,  $D_e''$ , is 1.16 volts.

siderably, both from Wurm's<sup>3</sup> experimental value, 1.69 volts and from Delbrück's<sup>4</sup> calculated 1.4 volts.

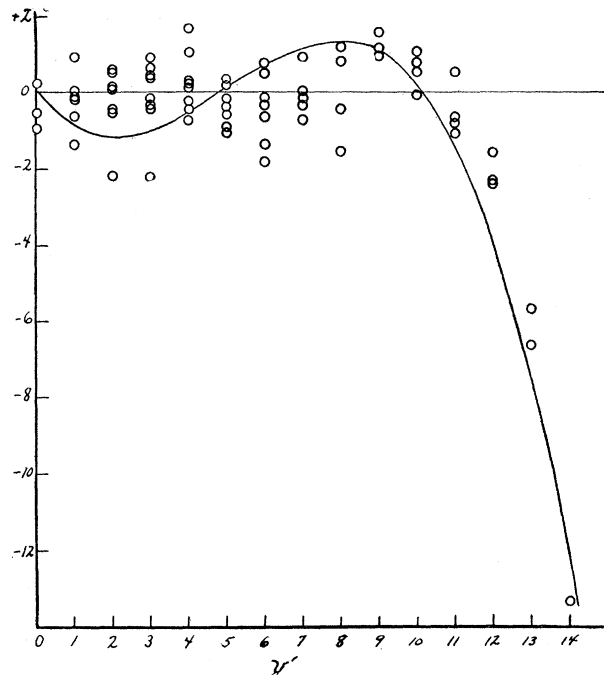


Fig. 3. Residuals of observed frequencies from Eq. (1). The curve represents Eq. (2).

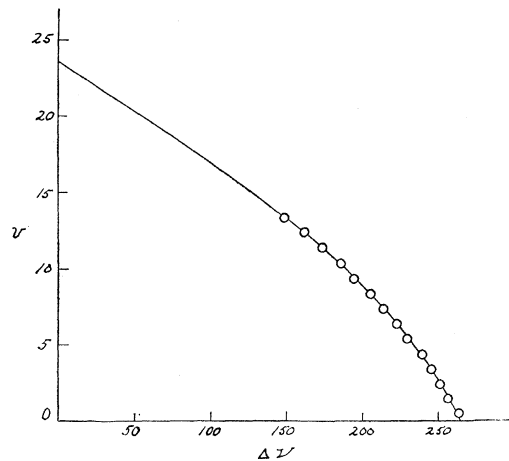


Fig. 4.  $\nu'$  vs.  $\Delta\nu$  plotted for upper level of green system to allow extrapolation according to Birge and Spomer. The curve follows Eq. (2).

Figs. 4 and 5 show, in two ways, how little extrapolation for  $D'$  is necessary, and give some idea of the accuracy of the result. In Fig. 4, following Birge and Spomer<sup>13</sup>  $\nu'$  is plotted against  $\Delta\nu$ , or as they call it,  $\omega$ , the energy

<sup>13</sup> Birge and Spomer, Phys. Rev. **28**, 259 (1926).



difference between successive vibrational levels, and  $D'$  is the area under the curve. In Fig. 5  $\Delta\nu$  is plotted against  $T'$  and the intercept on the  $T'$  axis is  $\nu_0 + D'$ . For convenience, a scale of the values of  $D_0''$  which would correspond

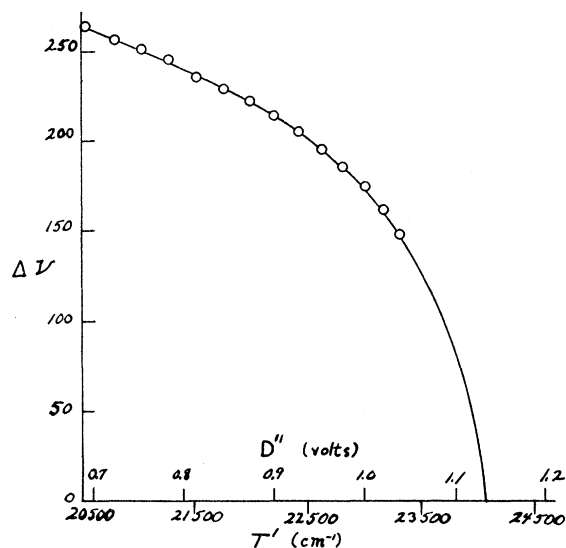


Fig. 5.  $\Delta\nu$  vs.  $T'$  plotted and extrapolated to dissociation following Eq. (2). Upper scale of abscissae represents values of  $D_0''$  which would be deduced from corresponding  $T'$  intercepts.

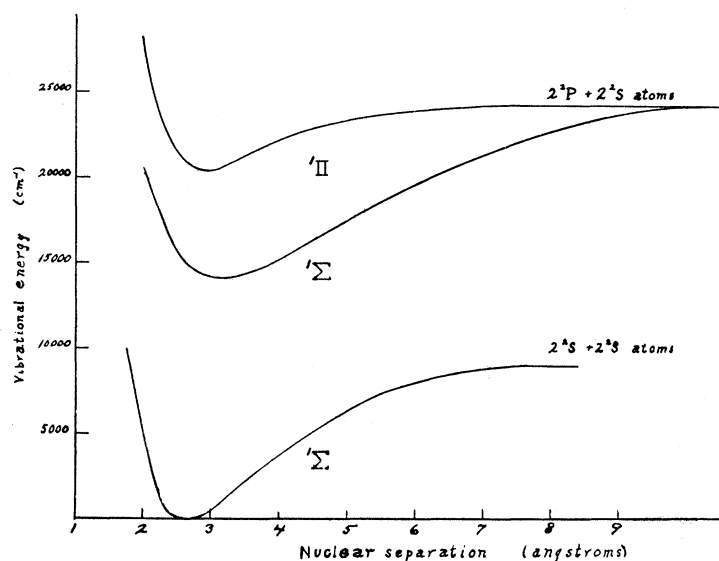


Fig. 6. Potential energy curves for the three accurately known levels of  $\text{Li}_2$ .

to various intercepts of the curve is inserted above the axis of  $T'$ . It is apparent that convergence has already been followed to within 0.1 volt of dissociation and that the value 1.14 volts can hardly be in error by more than about

0.03 volt. The curves shown in Figs. 4 and 5 are calculated on the basis of Eq. (2). The difference between Eqs. (1) and (2) would not show on the scale of these figures in the region where (1) is superior.

The potential energy curves in Fig. 6 were calculated, by the usual methods, on the basis of the data in Table II, which are the best now available for the constants of the lithium molecule.

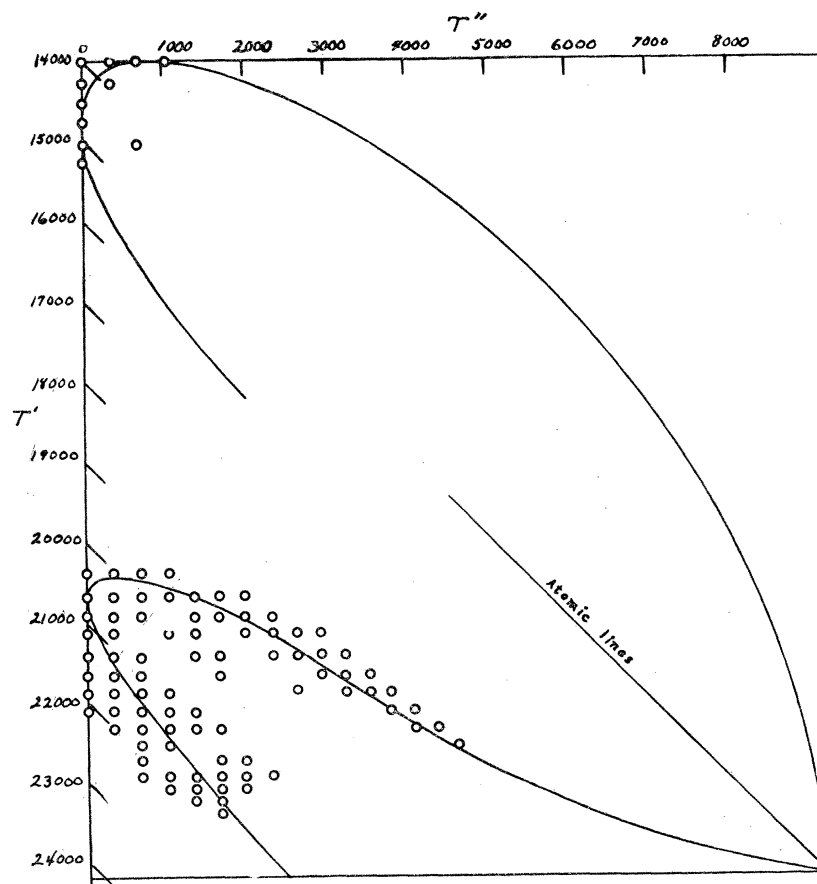


Fig. 7. Improved Franck-Condon diagram for the red and green systems. Circles represent observed bands; in the green system magnetic rotation, in the red system absorption bands. Lines of constant frequency are straight lines sloping at 45°.

TABLE II.

state	$T_e$	$\omega_e$	$\omega_e x_e$	$\omega_e y_e$	$B_0$	$r_e \cdot 10^8$	$D_0(\text{cm}^{-1})$	$D_0(\text{volts})$
ground $^1\Sigma$	0	351.60	2.590	0.0097	0.66914 <sup>8</sup>	2.67 <sup>8</sup>	9232	1.14
upper $^1\Sigma$	14070 <sup>7</sup>	253.2 <sup>7</sup>	1.5 <sup>7</sup>	—	0.495 <sup>7</sup>	3.12 <sup>7</sup>	10114	1.25
$^1\Pi$	20439.40	269.69	2.744	0.0637	0.55321 <sup>8</sup>	2.93 <sup>8</sup>	3738	0.46

All observed bands, and the calculated locus of maximum intensities are shown in Fig. 7 which is an improved form of Franck-Condon diagram. The

improvement consists in plotting  $T'$  and  $T''$ , the upper and lower energy terms, instead of  $v'$  and  $v''$ , the quantum numbers, as coordinates. There are several advantages to this method of plotting. In the first place, the frequency,  $\nu = T' - T''$ , of any band can be found by projecting the point representing it at  $45^\circ$  onto the  $T'$  axis. It also allows the representation of continua and of the atomic lines into which the systems converge and any number of systems can be plotted on one diagram. Moreover, the construction of the calculated locus of maximum intensities is much simpler as it involves merely plotting from two potential energy curves the heights of pairs of points with the same abscissae, and does not necessitate any calculation with vibrational quanta.

The bands of the red system as observed by Wurm<sup>7</sup> in absorption are also shown on Fig. 7, as is the calculated locus of maximum intensities for this system. The contrast between the richness of the magnetic rotation spectrum measurements and the meagreness of the absorption ones is very striking.

It will be noted that there must be an infrared edge to the absorption spectrum of  $\text{Li}_2$  like that observed by Loomis and Nile<sup>14</sup> in  $\text{Na}_2$ . It should come at about  $11000 \text{ cm}^{-1} = 9000\text{A}$ . We looked for it there but failed to find it, almost certainly because we were not able to get sufficient density of vapor.

The agreement between the calculated locus and the observed bands, especially in the right arm of the green system, is unusually good. We are inclined to attribute it to our having been able to follow the levels so close to convergence, so that the extreme right hand portions of the potential energy curves are better than was the case of sodium, for instance.

<sup>14</sup> Loomis and Nile, *Phys. Rev.* **32**, 873 (1928).

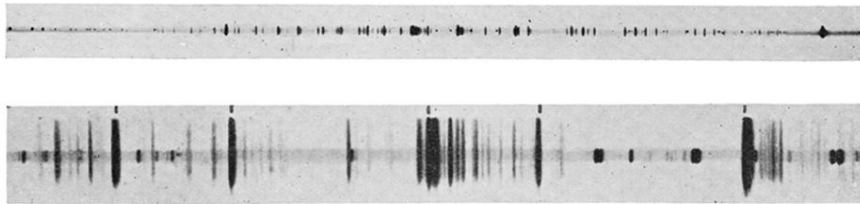


Fig. 2. a. Whole green magnetic rotation system of  $\text{Li}_2$ . b. Enlarged portion near origin.  
Short lines are iron comparison.